System modeling and identification in indicator dilution method for assessment of ejection fraction and pulmonary blood volume

Biomedical Signal Processing and Control 7 (2012) 640–648

Contents lists available at SciVerse ScienceDirect

Biomedical Signal Processing and Control

journal homepage: www.elsevier.com/locate/bspc

System modeling and identification in indicator dilution method for assessment of Ejection Fraction and Pulmonary Blood Volume

H.N. Bharath[a,*], K.M.M. Prabhu[a], H.H.M. Korsten[b], M. Mischi[c]

[a] Department of Electrical Engineering, Indian Institute of Technology, Madras 600036, India
[b] Department of Anaesthesiology, Catharina Hospital, Eindhoven, The Netherlands
[c] Signal Processing Systems Group, Department of Electrical Engineering, Eindhoven University of Technology, Eindhoven, The Netherlands

ARTICLE INFO

Article history:
Received 1 November 2011
Received in revised form 13 March 2012
Accepted 17 March 2012
Available online 8 April 2012

Keywords:
Parameter estimation
Least squares
Least absolute deviation
Indicator dilution method
Robust regression

ABSTRACT

Clinically relevant cardiovascular parameters, such as pulmonary blood volume (PBV) and ejection fraction (EF), can be assessed through indicator dilution techniques. Among these techniques, which are typically invasive due to the need for central catheterization, contrast ultrasonography provides a new emerging minimally invasive option. PBV and EF are then measured by a dilution system identification algorithm after detection of multiple dilution curves by an ultrasound scanner. In this paper, dilution systems are represented by parametric models. Since the measured indicator dilution curves (IDCs) are corrupted by measurement artifacts and outliers, the use of conventional least square error (LSE) estimator for estimating system parameters is not optimal. Different estimators are therefore proposed for estimating the system parameters. Comparison of these estimators with the LSE estimator in assessing EF and PBV is performed on simulated, in vitro and patient data. The results show that the proposed total least absolute deviation estimator (TLAD) outperforms other estimators. The measured IDCs are highly corrupted by noise, which affect the estimation of EF and PBV. Therefore, a two stage denoising method capable of removing outliers is also proposed for removing noise in IDCs.

1. Introduction

Indication dilution measurements are invasive in nature, which involve central catheterization of the patient [1]. After the injection of an indicator bolus, the indicator concentration is measured at a specific region of the circulatory system over a period of time to generate a time series, referred to as indicator dilution curve (IDC) [2]. The measured IDC is then analyzed for assessment of several cardiovascular parameters. Such parameters include cardiac output (CO), ventricular ejection fraction (EF) [3] and pulmonary blood volume (PBV), which are valuable indicators of cardiac preload.

The injection of an ultrasound contrast agent (UCA) bolus allows an IDC echographic measurement, resulting in a minimally invasive technique [4,5]. UCAs are micro-bubbles (of diameter from 1 to 10 μm) encapsulated in a shell of biocompatible material. When subjected to an ultrasonic beam, UCAs oscillate and backscatter a large part of the acoustic energy [6,7]. As a result, UCAs are easily detected by an ultrasound transducer. Their passage in a specific region-of-interest (ROI) over time can be detected by B-mode ultrasound imaging to derive an UCA IDC. Several IDCs can be measured in different ROIs and directly interpolated and interpreted by specific models for a minimally invasive quantification of PBV and CO [8,9]. An UCA bolus is injected into a peripheral (arm) vein and its movement through the cardiac chamber is tracked by a transthoracic ultrasound transducer. This will measure the acoustic intensity backscattered by the diluted UCA. A four-chamber view allows one to measure an IDC from each cardiac chamber. Fig. 1 shows an example of four-chamber view with three ROIs overlapped on the right ventricle (RV), left atrium (LA), and left ventricle (LV), respectively. In fact, estimation of EF and PBV requires identification of the dilution system between two sites of the circulatory system: LA and LV for EF, RV and LA for PBV [9,10].

To identify the dilution system using the measured acoustic intensity, a linear relationship between UCA concentration and detected acoustic intensity is necessary. It is shown in [9,11] that at low UCA concentration and low mechanical index (MI) of the ultrasound scanner, the relationship between UCA concentration and the detected acoustic intensity is linear. The use of specific contrast detection modes [12], such as power modulation, allows reducing UCA concentrations while increasing the image signal-to-noise ratio (SNR). Yet the SNR in IDC measurements is corrupted by several noise sources, comprising bad UCA mixing as well as measurement artifacts due to pressure variations and blood acceleration in the cardiac chambers [9]. For IDC data acquisition,

* Corresponding author. Tel.: +91 9444084711.
E-mail addresses: hn.bharath@gmail.com (H.N. Bharath), prabhu@ee.iitm.ac.in (K.M.M. Prabhu), erik.korsten@catharina-ziekenhuis.nl (H.H.M. Korsten), m.mischi@tue.nl (M. Mischi).

1746-8094/$ – see front matter © 2012 Elsevier Ltd. All rights reserved.
doi:10.1016/j.bspc.2012.03.006

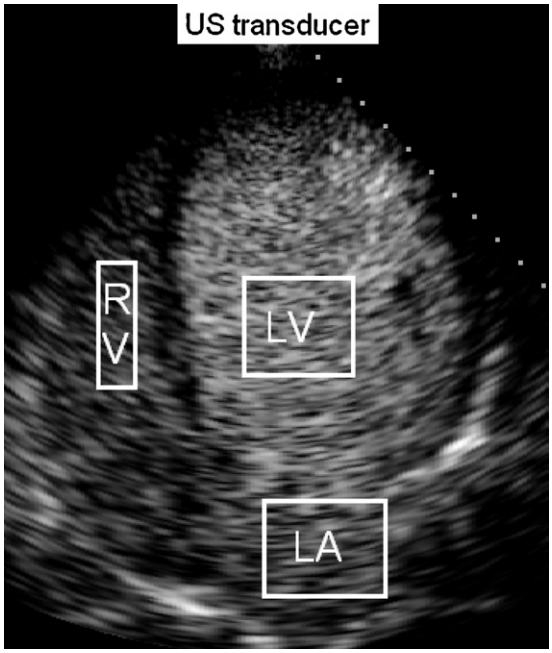

Fig. 1. Example of transthoracic four-chamber view with three ROIs overlapped on the right ventricle (RV), left atrium (LA), and left ventricle (LV), respectively.

the adopted ultrasound imaging mode was power modulation at 1.9 MHz with low mechanical index (MI = 0.1). The MI determines the mechanical interaction between ultrasound waves and UCA; therefore, a low MI helps in limiting the bubble disruption [13,14].

In this paper, the dilution systems are assumed to be linear and, therefore, the impulse response is sufficient to represent the entire dilution system. The estimated impulse response of the dilution system between the two detection sites can then be interpolated by specific models for the assessment of PBV and EF [10,15]. Once the IDCs are measured using the ultrasound scanner, linear dilution system can be identified through deconvolution techniques. In discrete domain, convolution can be viewed as a system of linear equations, $y = Ah$, where y, A and h are the output signal, circulant convolution matrix (composed of the input signal) and the dilution system impulse response, respectively. Then the estimation of the impulse response, h, is an inverse problem, whose least square error (LSE) solution is $\hat{h} = (A^TA)^{-1}A^Ty$. Although this approach is straight forward, the matrix A^TA will be nearly singular due to low SNR of the measured IDCs, and hence its inversion will be difficult. Singular value decomposition (SVD) can be used to find approximate inverse of A^TA, but this will result in poor estimates of EF and PBV.

An adaptive Wiener deconvolution filter is adopted to estimate the impulse response of the dilution system [10,15]. However, the Wiener deconvolution filter requires model interpolation of the estimated impulse response to calculate EF and PBV. This increases the variance of the estimated EF and PBV. Also at low SNR, Wiener filter acts as a low-pass filter [16]. As a result, the model interpolation of the impulse response is inaccurate. Besides, the model interpolation will be inaccurate when the frequency component of the input IDC is lower than those representing the transfer function of the dilution system. Since the estimation of EF and PBV depends on the quality of model interpolation of the estimated impulse response, this may result in erroneous assessment of EF and PBV.

To overcome the problems associated with the Wiener filter, a new parametric deconvolution method was proposed [16]. This method employs specific parametric models that represent the dilution system. As a result, the system identification reduces to finding a few system parameters rather than all the frequency components of the dilution system transfer function. In the parametric deconvolution method, system parameters are estimated without model interpolation of the impulse response; therefore, the estimated system parameters show less variance. This improves the measurement of EF and PBV. In this method, the system parameters are identified by minimizing the squared error between the measured and the estimated output IDC of the dilution system represented by the parametric model. In [16], a low-pass finite impulse response (FIR) filter is used for denoising the measured IDCs and the system parameters are estimated using an LSE estimator. It is observed that the measured IDCs contain outliers and nonlinearities. LSE is not a robust estimator in the presence of outliers and also the FIR filter is not capable of removing outliers. As a result, the estimated EF and PBV will not be robust and may result in poor estimates.

In order to overcome the problem with LSE estimator, we propose many robust estimators which can take care of outliers present in the IDCs. In this paper, the low-pass FIR filter proposed in [16] for removal of the IDC outliers is replaced by a two stage denoising method. The remainder of the paper is organized as follows: In Section 2, the modeling of the dilution system is described. In Section 3, different estimators used for system identification are proposed. The denoising methods used and the LA IDC attenuation compensation are discussed in Section 4. A comparison of the proposed estimators using a set of measurements in patients is presented in Section 5. Conclusions and future course of work are discussed in Section 6.

2. System modeling

For EF measurements, the LV dilution system is described by a mono-compartment model [16], whose impulse response to a rapid contrast injection is given by an exponential decay signal

$$h(t) = c_0 e^{(-t/\tau)}, \tag{1}$$

where τ is the time constant of the system and c_0 is the initial contrast concentration at time $t = 0$. Once the LV dilution system parameters, c_0 and τ, are estimated, EF is calculated as

$$EF = 1 - \frac{h_{i+1}}{h_i} = 1 - e^{\triangle t/\tau}, \tag{2}$$

where h_i and h_{i+1} are contrast concentrations at two subsequent systole and $\triangle t$ is the cardiac period [3].

For PVB measurements, the transpulmonary dilution system between RV and LA is modeled as local density random walk (LDRW) model [16], with impulse response,

$$C(t) = \frac{m}{Q} e^{\lambda} \sqrt{\frac{\lambda}{2\pi\mu t}} e^{-(\lambda/2)((t/\mu)+(\mu/t))}, \tag{3}$$

where m is the injected dose of contrast, Q is the flow, μ is the mean transmit time (MTT) that the contrast takes to cover the distance between the injection and the detection sites after an impulse injection and λ is a parameter related to the diffusion constant of the system that determines the IDC skewness [9,8]. Once the LDRW parameters Q, μ and λ are estimated, the volume between two sites is given by

$$PBV = Q\mu. \tag{4}$$

Here the flow Q, which corresponds to the CO used in the PBV calculation, is not assessed from dilution system identification, but only the parameter μ is derived from the LDRW model representation of the dilution system. The flow Q is calculated by echo-Doppler time integration in the aorta [17].

2.1. LV dilution system

(1) *Model-1*

The LV dilution system transfer function in the Laplace domain is given as

$$H(s) = \frac{c_0}{s + (1/\tau)}. \tag{5}$$

This continuous-time transfer function is mapped into an equivalent discrete-time transfer function using the bilinear transformation as

$$H_1(z) = \frac{(c_0/((1/\tau) + (2/T)))(1 + z^{-1})}{1 + (((1/\tau) - (2/T))/((1/\tau) + (2/T)))z^{-1}}, \tag{6}$$

where T represents the sampling period. The time-domain representation of (6) is given by

$$y(n) = \frac{c_0}{((1/\tau)+(2/T))}(x(n)+x(n-1)) - \left(\frac{(1/\tau)-(2/T)}{(1/\tau)+(2/T)}\right) y(n-1), \tag{7}$$

where y and x are the output and the input of the system, respectively.

(2) *Model-2*

The LV dilution system impulse response $h(t)$ is discretized by sampling at T, which is the sampling period of the input and output IDCs. The discrete–time system and its Z-transform is given by

$$h_2(nT) = c_0 e^{(-(nT/\tau))}, \tag{8}$$

$$H_2(z) = \frac{c_0}{1 - (e^{-(T/\tau)})z^{-1}}. \tag{9}$$

The time-domain representation of (9) is given as

$$y(n) = c_0 x(n) + (e^{-(T/\tau)})y(n-1). \tag{10}$$

Both the systems, namely, Model-1 and Model-2, can be represented in a matrix form as

$$y = Ah, \tag{11}$$

where A is a circulant convolution matrix formed from the input signal x.

2.2. Transpulmonary dilution system

Due to the complexity of the Laplace transform of the LDRW model, the impulse response $c(t)$ is simply discretized by sampling it at T, as in the case of Model-2, which is given by

$$C(nT) = \frac{m}{Q} e^{\lambda} \sqrt{\frac{\lambda}{2\pi\mu nT}} e^{-(\lambda/2)((nT/\mu)+(\mu/nT))}, \tag{12}$$

and its matrix representation is given as

$$y = Ac. \tag{13}$$

3. System identification

Once the system has been modeled as in Section 2, the problem of system identification reduces to the estimation of system parameters. Direct estimation of the system parameters has two advantages: (1) the EF and PBV are obtained directly as in (2) and (4), without interpolating the system impulse response and (2) the estimated system parameter will have less variance. Since the system parameters are not linearly related to the system input, any non-linear optimization technique such as the Nelder Mead Simplex Method can be used to estimate the system parameters.

The system parameters are obtained by minimizing an error function over the system parameters.

$$\widehat{\Omega} = \min_{\Omega} f(x, r, \Omega), \tag{14}$$

where f is the error function, x is the measured system input, r is the measured output and Ω is the set of system parameters. In this paper, we consider eight estimators corresponding to different error functions for the estimation of EF and PBV.

Let y be the output of the system for an input x. For EF measurements, y is obtained as in (7) or (10) and for PBV measurements y is obtained as in (13).

(1) *Least square error (LSE)*:

This is the most widely used error function, where the squared error between the measured and the estimated output is minimized over system parameters

$$\widehat{\Omega} = \underset{\Omega}{\mathrm{argmin}} \sum_{i=1}^{N} (y(i) - r(i))^2. \tag{15}$$

If the noise is stationary and has a normal distribution, LSE corresponds to the maximum likelihood criterion [18]. However, the measured IDCs are corrupted by non-stationary noise along with non-linearities in the measurements and, therefore, the LSE estimation deviates from the maximum likelihood criterion.

(2) *Least absolute deviation (LAD)*:

Here the sum of the absolute error between the measured and the estimated output is minimized as given by

$$\widehat{\Omega} = \underset{\Omega}{\mathrm{argmin}} \sum_{i=1}^{N} |y(i) - r(i)|. \tag{16}$$

LAD is more robust to outliers in data than LSE. Since there are many outliers present in the measured IDCs, LAD will be a better choice than LSE for EF and PBV estimation.

(3) *Iteratively reweighed least squares (IWLS)*

In IWLS, the weighted LSE, given in (17), is solved iteratively:

$$\widehat{\Omega}^{(k+1)} = \underset{\Omega}{\mathrm{argmin}} \sum_{i=1}^{N} W^{(k+1)}(i)|y(i) - r(i)|^2. \tag{17}$$

At each iteration, the weights $W(i)$ are updated based on the residual error, $\epsilon(i)$ from the previous iteration [19]. Here, we have used a bi-square weight function to update the weights, which is given by

$$W(i) = \begin{cases} (1 - \epsilon^2(i))^2, & |\epsilon(i)| < 1 \\ 0, & |\epsilon(i)| \geq 1 \end{cases}, \tag{18}$$

The weights are not used for the first iteration and the algorithm stops when the relative change in the system parameters is less than some fixed constant.

(4) *Huber function regression (HFR)*:

This acts as an hybrid between LSE and LAD. For an error residue ϵ, the Huber function is defined as

$$H(\epsilon) = \begin{cases} \frac{1}{2}\epsilon^2, & |\epsilon| \leq \rho \\ \rho|\epsilon| - \frac{1}{2}\rho^2, & |\epsilon| > \rho \end{cases}. \tag{19}$$

With a slight modification to Huber function given in (19), a new error function, referred to as modified Huber function regression (MHFR), is obtained as

$$H_1(\epsilon) = \begin{cases} \epsilon^2, & |\epsilon| \leq \rho \\ \rho|\epsilon| + \frac{1}{2}\rho^2, & |\epsilon| > \rho \end{cases}. \tag{20}$$

In the modified Huber function regression (MHFR), large errors are given greater weight than in HRF. The system parameters are obtained by minimizing the Huber function.

(5) *Iterative reweighed least absolute deviation (IRLAD)*:

A weighted LAD, given in (21), is solved repeatedly with weights being updated after each iteration based on the residual error:

$$\widehat{\Omega}^{(k+1)} = \underset{\Omega}{\operatorname{argmin}} \sum_{i=1}^{N} W^{(k+1)}(i)|y(i) - r(i)|. \tag{21}$$

At each iteration, the weights are updated using a Cauchy's weight function

$$W(i) = \frac{1}{1+\epsilon^2(i)}, \quad \text{for } i = 1, 2, \ldots, N. \tag{22}$$

The iteration is carried out n times and in this paper we have used $n = 3$.

(6) *Total least squares (TLS)*:

Both the measured IDCs (input and output) are subjected to random noise and the error model is given by

$$x = x_o + \delta \tag{23}$$

$$y = y_o + \eta \tag{24}$$

where x_o and y_0 are the true values of the input and output, respectively, δ and η are additive noise. The system output, y_0 is given as a function of x_o and system parameters, Ω.

$$y_o = f(x_o, \Omega) \tag{25}$$

or

$$y = f(x - \delta, \Omega) + \eta. \tag{26}$$

The total least squares formulation for system parameter identification [20] is given as

$$\widehat{\Omega} = \underset{\Omega,\delta}{\operatorname{argmin}} \sum_{i=1}^{N} (y(i) - f(x(i) - \delta(i), \Omega))^2 + \delta(i)^2. \tag{27}$$

The problem in (27) can be solved using Orthogonal Distance Regression approach [20]. In this method, the number of unknown variables to be estimated is large, as the minimization is done over both Ω and δ. To overcome this problem, the TLS represented in (27) is reformulated, such that the minimization is done over the system parameter Ω only.

Let us consider linear regression with errors in the measurement matrix. The measurement, b is modeled as

$$b = (D + E)x + \eta, \tag{28}$$

where D is the measurement matrix, E is the unknown perturbation matrix (errors in measurement) and η is the unknown perturbation vector (additive error at output). In TLS approach, we seek the values of x, η and E such that the perturbations E and η have minimum L_2 norm with the constraint that (28) is consistent, which is given by

$$\hat{x} = \underset{E,x,\eta}{\operatorname{argmin}} \{\|E\|_2^2 + \|\eta\|_2^2 : b = (D + E)x + \eta\}. \tag{29}$$

By minimizing (29) with respect to E and η, the problem can be reformulated as a minimization problem in variable x [21] as

$$\hat{x} = \underset{x}{\operatorname{argmin}} \frac{\|Dx - b\|_2^2}{\|x\|_2^2 + 1}. \tag{30}$$

Based on (7) or (10), the TLS formulation given in (30) is applied for estimating the system parameters of the LV dilution system as

$$\hat{\Omega} = \underset{\Omega}{\operatorname{argmin}} \frac{\|y - r\|_2^2}{\|\alpha\|_2^2 + 1}, \tag{31}$$

where y is the estimated system output, r is the actual measured noisy system output and α is a vector of parameters. For Model-1 and Model-2, α is determined from (7) and (10), respectively, as

$$\alpha = \begin{cases} \left[\dfrac{c_0}{((1/\tau)+(2/T))}, \dfrac{((1/\tau)-(2/T))}{((1/\tau)+(2/T))}\right]^T, & \text{for Model-1} \\ [c_0, e^{T/\tau}]^T, & \text{for Model-2.} \end{cases}$$

Since there are many outliers present in IDCs, L_1 norm is more robust than L_2 norm, so the L_2 norm error, $\|y - r\|_2^2$ in (31) is replaced by L_1 norm error, $\|y - r\|_1$. This modified formulation is referred to as total least absolute deviation (TLAD)

$$\hat{\Omega} = \underset{\Omega}{\operatorname{argmin}} \frac{\|y - r\|_1}{\|\alpha\|_2^2 + 1}. \tag{32}$$

The system parameters are estimated by minimizing the error functions described above. In this paper, we have used Nelder–Mead simplex method [22] to minimize the error functions. Nelder–Mead simplex method requires initial values of the system parameters to start. In LV dilution system identification, $\Omega = [c_0, \tau] = [0.05, 2]$ is used as the initial value. MHFR is sensitive to the chosen initial values. Therefore, the system parameter estimated by LAD is used as an initial parameter for the MHFR. In transpulmonary dilution system identification, the initial value used for optimization is, $\Omega = [\lambda, \mu, a_0] = [5, 10, 20]$. The initial values, τ and μ used in system identification are based on the average values observed in patients. The initial values of other parameters, c_0, λ and a_0 are selected empirically.

4. Pre-processing steps

The measured signal is corrupted by additive noise,

$$y = x + \eta, \quad y,\ x,\ \eta \in \mathbb{R}^n,$$

where y is the measured signal, x is the actual signal and η is the additive noise. In this paper, the noise is removed by a two stage denoising technique. In the first stage, high frequency noise is removed from corrupted IDC using a finite impulse response (FIR) filter or total variation (TV) denoising method. In the second stage, FIR filtered or TV denoised signals are smoothed using a local regression technique called robust locally weighted regression and smoothing scatterplots (Rloess) [23]. Rloess is used here mainly to remove outliers present in the IDC. For FIR filtering, we have used a 5-tap low-pass FIR filter with a normalized cut-off frequency of 0.025 and the normalization is done with respect to the sampling frequency.

4.1. Total variation (TV) denoising

TV of a signal is a measure of change between the signal values. For a discrete signal with N samples, TV is defined as

$$TV(x) = \sum_{n=2}^{N} |x(n) - x(n-1)|, \tag{33}$$

which can also be written as,

$$TV(x) = \|Dx\|_1, \tag{34}$$

where D is the difference operator. Denoising is done by minimizing an objective function with a TV constraint given by

$$\hat{x} = \min_x J(x) = \min_x \|y - x\|_2^2 + \lambda \|Dx\|_1, \tag{35}$$

where y is the measured noisy signal, $\hat{x}$ is the denoised signal and λ is the regularization parameter which controls the smoothness of the signal. For larger noise levels, larger values of λ are required. It is

difficult to solve the problem presented in (35) because of the non-smooth part ($\lambda \parallel Dx \parallel_1$). To overcome this difficulty, we use a dual approach proposed in [24,21]. The dual formulation of the problem in (35) is given by

$$\hat{x} = \max_{|z|\leq 1} \min_{x} \|y - x\|_2^2 + \lambda z^T Dx, \tag{36}$$

where z is an auxiliary variable and z^T is its transpose. The dual problem given in (36) can be solved iteratively using gradient-based algorithm and majorization–minimization method [25,26]. The update equations for x and z at each iteration are given by

$$\begin{aligned} x^{(k+1)} &= y - \frac{\lambda}{2} D^T z^{(k)} \quad \text{and} \\ z^{(k+1)} &= clip\left(z^{(k)} + \frac{2}{\alpha\lambda} Dx^{(k+1)}, 1\right), \end{aligned} \tag{37}$$

where D^T is the transpose of D and *clip* is a clipping function defined below:

$$clip(b, 1) = \begin{cases} b, & |b| \leq 1 \\ sign(b), & |b| > 1 \end{cases}. \tag{38}$$

x and z are updated iteratively till the relative change in x between the iterations is less than a fixed constant, δ, i.e., $\|x^k - x^{k-1}\|_2^2 < \delta$ (we have used $\delta = 0.0001$).

4.2. Robust locally weighted regression and smoothing scatterplots (Rloess)

In Rloess, denoising is done based on the assumption that original signal is smooth. This assumption allows us to use neighborhood points of (x_n, y_n) to estimate the denoised signal, $\hat{y}_n$, and, therefore, the name locally weighted regression. This algorithm is described below.

Let us define a weighting function, W with properties:

(a) $W(x) > 0$ for $|x| < 1$.
(b) $W(-x) = W(x)$.
(c) $W(x)$ is a non increasing function for $x \geq 0$.
(d) $W(x) = 0$ for $|x| \geq 1$.

If l is the half length of the local span window, then the weights are defined as

$$w_k(x_n) = W((x_k - x_n)/l), \quad \text{for } k = 1, 2, \ldots, N. \tag{39}$$

(1) For each n, find the estimate, $\alpha(x_n) = [\alpha_0, \alpha_1, \alpha_2]$ of a second order polynomial regression. The $\alpha(x_n)$'s are estimated using a weighted least squares fit with weights defined as in (39):

$$\alpha(x_n) = \arg\min_{\alpha} \sum_{k=1}^{N} w_k(x_n)(y_k - \alpha_0 - \alpha_1 x_k - \alpha_2 x_k^2)^2. \tag{40}$$

The smoothed or denoised signal value at x_n is $(x_n, \hat{y}_n)$, where $\hat{y}_n$ is the fitted regression value given as

$$\hat{y}_n = \alpha_0 + \alpha_1 x_n + \alpha_2 x_n^2 = \sum_{k=1}^{N} r_k(x_n) y_k, \tag{41}$$

where $r_k(x_n)$ is independent of the signal y. The estimates, $\hat{y}_n$ are calculated for all $n = 1, 2, \ldots, N$, to obtain a smooth signal $\hat{y}$. However, this estimate is not robust and is sensitive to outliers. To make this more robust to outliers, the following steps are applied:

(2) Let B be a bi-square weight function defined as

$$B(x) = \begin{cases} (1 - x^2)^2, & |x| < 1 \\ 0, & |x| \geq 1 \end{cases}. \tag{42}$$

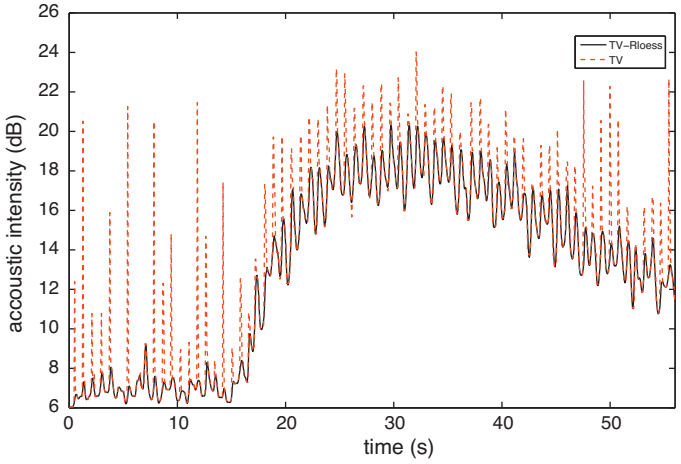

Fig. 2. LV IDC after denoising using single stage TV denoising and two stage TV-Rloess methods.

Let ϵ_n be the residual error, i.e., $\epsilon_n = y_n - \hat{y}_n$. Then, the robustness weights are defined as

$$\rho_n = B\left(\frac{\epsilon_n}{6s}\right), \tag{43}$$

where s is the median of the residual error, ϵ.

(3) The new estimate $\hat{y}$ is computed as described in step 1, but with a new weight $\rho_n w_k(x_n)$ at each (x_k, y_k).

(4) Steps 2 and 3 are repeated till the relative change in the estimated $\hat{y}$ between iterations is less than a fixed value.

The weight function used in step 1 is tri-cubic weights, defined as

$$W(x) = \begin{cases} (1 - x^3)^3, & |x| < 1 \\ 0, & |x| \geq 1 \end{cases}. \tag{44}$$

4.3. LA IDC attenuation compensation

All the measured IDCs are obtained by software Q-Lab® (Philips Healthcare, Andover) for acoustic quantification. The returned data series are given in decibel (dB). However, for application of the indicator dilution theory by system identification, IDCs must be represented as acoustic intensities, since the UCA concentration is linearly proportional to acoustic intensities. Therefore, once the IDCs in dB are denoised, they are converted to acoustic intensities, $x_i = 10^{(x/10)}$. In fact, due to the multiplicative characteristics of IDC noise [8], denoising in the logarithmic domain seems a

Table 1
Mean (top) and variance (bottom) of the estimate τ using LAD, LSE, TLAD, TLS, HRF and MHFR estimators for different values of τ.

Actual τ	LAD	LSE	MHFR	HFR	TLAD	TLS
0.4	0.4182	0.4323	0.4257	0.4237	0.4394	0.4493
	0.0033	0.0060	0.0041	0.0046	0.0027	0.0053
0.5	0.5089	0.5165	0.5137	0.5120	0.5236	0.5292
	0.0025	0.0054	0.0033	0.0038	0.0024	0.0051
0.7	0.7015	0.7185	0.7042	0.7049	0.7106	0.7201
	0.0031	0.0068	0.0034	0.0042	0.0030	0.0066
1.0	1.0017	1.0095	1.0013	1.0036	1.0061	1.0146
	0.0021	0.0055	0.0030	0.0033	0.0021	0.0055
1.3	1.3049	1.3039	1.3090	1.3065	1.3082	1.3076
	0.0028	0.0084	0.0036	0.0045	0.0028	0.0084
1.9	1.8946	1.8983	1.8956	1.8952	1.8963	1.9010
	0.0018	0.0081	0.0030	0.0035	0.0017	0.0081
3.0	2.9996	2.9973	2.9982	2.9981	3.0007	2.9993
	0.0019	0.0098	0.0030	0.0036	0.0019	0.0098
6.0	6.0094	6.0157	6.0147	6.0111	6.0103	6.0175
	0.0036	0.0190	0.0064	0.0088	0.0036	0.0190

Table 2
Mean (top) and variance (bottom) of the estimate μ using LAD and LSE estimators for different values of μ.

Actual μ	2	4	6	8	10	12	14	16
LAD	1.9953	3.9943	5.9977	8.0033	10.0000	11.9974	13.9427	15.9783
	0.0036	0.0088	0.0042	0.0078	0.0049	0.0057	0.1673	0.1062
LSE	1.9893	4.0004	6.0002	8.0038	10.0005	11.9493	13.8049	14.7760
	0.0098	0.0069	0.0080	0.0043	0.0090	0.2900	1.5321	11.3662

proper choice, resulting in additive noise. The LA IDC measurement, which is used for assessment of both EF and PBV, suffers from non-stationary distortion due to acoustic intensity attenuation by LV contrast dilution. Also, the LA IDC suffers from stationary attenuation due to tissue between the transducer and LA region, the tissue can be seen in Fig. 1. The compensation for LA IDC is given by [16]

$$I_{LA}(t) = \hat{I}_{LA} e^{4arf} \cdot \left(\frac{\hat{I}_{LV_{max}} e^{-4arf}}{b\hat{I}_{LA_{max}}} \right)^{(I_{LV}(t)/\hat{I}_{LV_{max}})}, \quad (45)$$

where I_{LA}, $\hat{I}_{LA}$ and $\hat{I}_{LV}$ are the real LA IDC, and the measured LA IDC and LV IDC, respectively. The LA attenuation compensation in (45) is based on the assumption that b, the ratio between $I_{LA_{max}}$ and $I_{LV_{max}}$, is equal to one. The parameters a, r and f are the attenuation coefficient of the tissue, the distance between LV and LA ROI and the central frequency of ultrasonic pulses, respectively. As in [16], the values of these parameters are $a = 0.3\,\mathrm{dB\,cm^{-1}\,MHz^{-1}}$, $r = 5$ cm, and $f = 1.9$ MHz. The LA IDC attenuation compensation is divided into two parts, the stationary part given by e^{4arf} and the non-stationary part, $(\hat{I}_{LV_{max}} e^{-4arf}/b\hat{I}_{LA_{max}})^{(I_{LV}(t)/\hat{I}_{LV_{max}})}$. Firstly, the stationary compensation is done, while the non-stationary compensation is done only if the peak LA IDC is larger than the peak of LV IDC after stationary compensation.

5. Results and discussion

To compare the behavior of the estimators for EF estimation, simulation is performed in the presence of noise. LA IDC is generated using LDRW model curve with $\mu = 8$. LV IDC is generated with LA IDC as input to the LV dilution model with different values of τ. The values of τ used corresponds to EF ranging from 10% to 80% for a heart rate of 90 bpm. For both LA IDC and LV IDC, Gaussian noise is added (SNR = 12 dB), whose variance is proportional to the amplitude of the IDCs [8]. Mean and variance of the estimated τ for 100 different noise sequences is given in Table 1. Although the mean value of τ is almost the same for all the estimators, LAD and TLAD estimators have the least variance of τ, followed by MHFR and HRF and TLS estimators. LSE has the highest variance among all the estimators.

The performance of LAD and LSE estimators in the estimation of the PBV is compared by simulation in the presence of noise. RV IDC is generated by convolving a rectangular impulse of 1 s that stimulates the injection function and a LDRW model curve ($\lambda = 3$ and $\mu = 5$) that stimulates the impulse response between arm and the RV. The RV IDC is then convolved with a LDRW model curve with $\lambda = 7$ and μ ranging from 2 s to 16 s to generate LA IDCs. The values of μ considered, covers the entire range measured in patients. For both RV IDC and LA IDC, Gaussian noise is added (SNR = 12 dB), whose variance is proportional to the amplitude of the IDCs [8]. Mean and variance of the estimated μ for 100 different noise sequences is given in Table 2. Simulation results show that the variance of the estimated μ is less in LAD estimator compared to LSE estimator.

To assess the clinical feasibility of these methods, IDCs were measured by a Philips Sonos 5500 scanner (Philips Healthare, Andover), equipped with transthoracic S3 probe, after the injection of a 0.05 mL bolus of SonoVue® UCA (Bracco Suisse, Geneva) diluted in 5 mL of saline (0.9% NaCl) [27].

The EF estimates of dilution methods are tested using a set of 82 measurements in patients with EF ranging from 10% to 80%. The measurements are compared with biplane echocardiographic assessments after contrast opacification of the LV (an average of three measurements). The use of contrast enhancement allows a better delineation of the endocardial wall, leading to improved accuracy of the biplane method, with reduced intra- and inter-observer variabilities of the measurement [28,29]. The measurements were performed at the Catharina Hospital in Eindhoven, The Netherlands. All the patients provided informed written consent.

Comparisons of different estimators and denoising techniques were done based on 4 parameters:

(1) Mean absolute deviation (MAD) of the difference between EF estimates by the bi-plane method and the dilution method:

$$MAD(x) = mean(|X - mean(X)|). \quad (46)$$

(2) Standard deviation (SD) of the difference between EF estimates by the bi-plane method and the dilution method.
(3) Correlation coefficient (CC) between EF estimates by the bi-plane method and the dilution method.

Table 3
MAD, SD, correlation and bias values of the error between EF estimates by biplane method and the parametric deconvolution method using LSE, LAD, MHFR HRF, IRLAD, TLAD, TLS estimators. Both LA and LV IDC are denoised using FIR filter. All the EF estimates are based on Model-1.

	LAD	LSE	MHFR	HFR	IRLAD	TLAD	TLS
MAD	11.4725	15.0982	9.8963	11.6057	11.4328	8.6025	11.6417
SD	15.4234	19.8174	13.4031	15.4158	15.4374	11.9032	15.3694
Corr	0.7070	0.5889	0.7185	0.7053	0.7073	0.7162	0.6697
Bias	13.1615	17.8977	10.5966	13.4101	12.7851	7.1807	13.6403

Table 4
MAD, SD, correlation and bias values of the error between EF estimates by biplane method and the parametric deconvolution method using LSE, LAD, MHFR HRF, IRLAD, TLAD, TLS estimators. Both LA and LV IDC are denoised using TV denoising method. All the EF estimates are based on Model-1.

	LAD	LSE	MHFR	HFR	IRLAD	TLAD	TLS
MAD	10.8958	14.6143	10.2553	11.1644	11.2719	8.8928	10.5598
SD	15.3194	19.4656	14.4912	15.2726	15.8109	12.2734	14.2007
Corr	0.6492	0.5947	0.6569	0.6915	0.6352	0.6836	0.6630
Bias	10.8048	18.2252	9.2675	12.2658	10.2478	5.6540	12.5437

Table 5
MAD, SD, correlation and bias values of the error between EF estimates by biplane method and the parametric deconvolution method using LSE, LAD, MHFR HRF, IRLAD, TLAD, TLS estimators. Both LA and LV IDC are denoised using Rloess denoising method. All the EF estimates are based on Model-1.

	LAD	LSE	MHFR	HFR	IRLAD	TLAD	TLS
MAD	10.4528	12.6153	9.6248	10.7296	10.4670	8.5616	9.6323
SD	14.8571	17.1073	12.7341	14.9651	14.8871	11.6626	12.7286
Corr	0.6644	0.6331	0.7091	0.6967	0.6684	0.7202	0.7104
Bias	9.6361	13.1996	7.7468	10.9143	9.4000	5.1422	9.6296

Table 6
MAD, SD, correlation and bias values of the error between EF estimates by biplane method and the parametric deconvolution method using LSE, LAD, MHFR HRF, IRLAD, IRLS, TLAD, TLS estimators. Both LA and LV IDC are denoised using two stage FIR-Rloess denoising method. All the EF estimates are based on Model-1.

	LAD	LSE	MHFR	HFR	IRLAD	IRLS	TLAD	TLS
MAD	10.0377	11.655	9.2764	9.7430	10.1569	10.2391	8.8741	9.7895
SD	14.0974	16.3087	12.5089	12.9283	14.4434	13.8128	12.1550	13.2544
Corr	0.6778	0.6304	0.7146	0.7369	0.6716	0.6683	0.6957	0.6782
Bias	8.5396	11.6162	6.9697	9.4705	8.0461	3.7200	5.1030	8.7926

Table 7
MAD, SD, correlation and bias values of the error between EF estimates by biplane method and the parametric deconvolution method using LSE, LAD, MHFR HRF, IRLAD, IRLS, TLAD, TLS estimators. Both LA and LV IDC are denoised using two stage TV-Rloess denoising method. All the EF estimates are based on Model-1.

	LAD	LSE	MHFR	HFR	IRLAD	IRLS	TLAD	TLS
MAD	9.1023	11.3735	8.7669	10.4091	8.7749	10.6977	8.5890	9.5542
SD	12.3349	15.5278	11.8045	14.6833	12.0505	14.6354	11.9145	12.9265
Corr	0.7185	0.6312	0.7352	0.6788	0.7337	0.6551	0.7042	0.6702
Bias	8.2662	11.3106	7.0053	10.3255	7.9044	5.0571	5.4130	8.2190

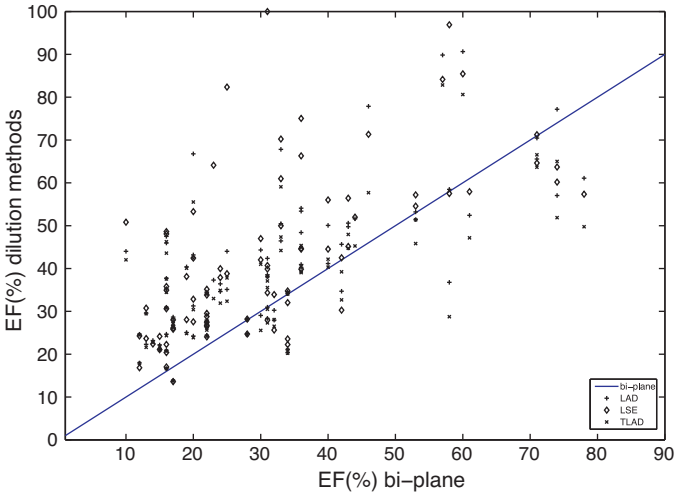

Fig. 3. EF (percentage units) measurements performed by the LSE, LAD and TLAD estimators on 82 measurements in patients. The line represents the same measurements made by the echocardiographic biplane method.

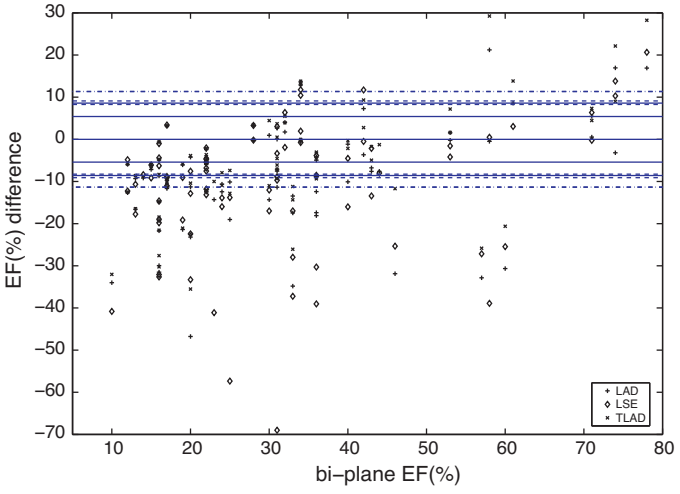

Fig. 4. Bland–Altam plot of the comparison between the LSE (dot-dashed lines), LAD (dashed lines) and the TLAD (continuous lines) with the echocardiographic biplane method after contrast opacification of the LV. The lines indicate the average and standard deviation interval.

(4) Bias, which is the mean of the difference between EF estimates by the dilution method and the biplane method.

The values of MAD, SD, CC and Bias for different estimators (LAD, LSE, MHFR, HFR, IRLAD, IRLS, TLS and TLAD) are provided in Tables 3–7, for different denoising methods, namely, FIR denoising, TV denoising, Rloess denoising, two stage FIR and Rloess denoising and two stage TV and Rloess denoising. The results shown in Tables 3–7 are based on Model-1.

FIR and TV denoising methods are not capable of removing outliers present in IDC, so the MAD and SD are higher as shown in Tables 3 and 4. With two stage denoising methods FIR-Rloess or TV-Rloess, the outliers are removed as shown in Fig. 2. This improves the EF estimation and results in lower values of MAD and SD, which is evident from Tables 6 and 7. Even though single stage denoising using Rloess method removes outliers, it performs poorer when compared to the two stage denoising method.

It is well known that LAD is a better estimator than LSE in the presence of outliers. Although denoising removes the main outliers from the IDCs, small residual noise remains which may become significant when the IDC is converted from dB into acoustic intensities, forming new outliers. Therefore, LAD, MHFR, IRLAD and TLAD give better EF estimates. HFR and IRLS, which are robust estimators, perform better than LSE.

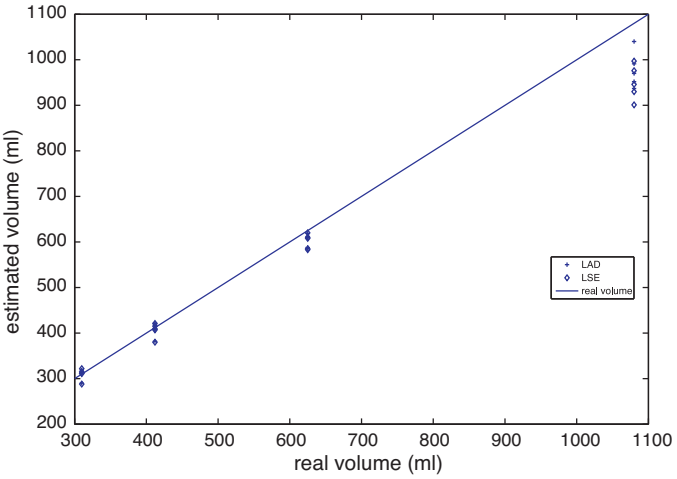

Fig. 5. In vitro volume measurements for four different volumes by LSE and LAD estimators. The results are the average of the volume estimates for four different flows, going from 1 to 5 L/min.

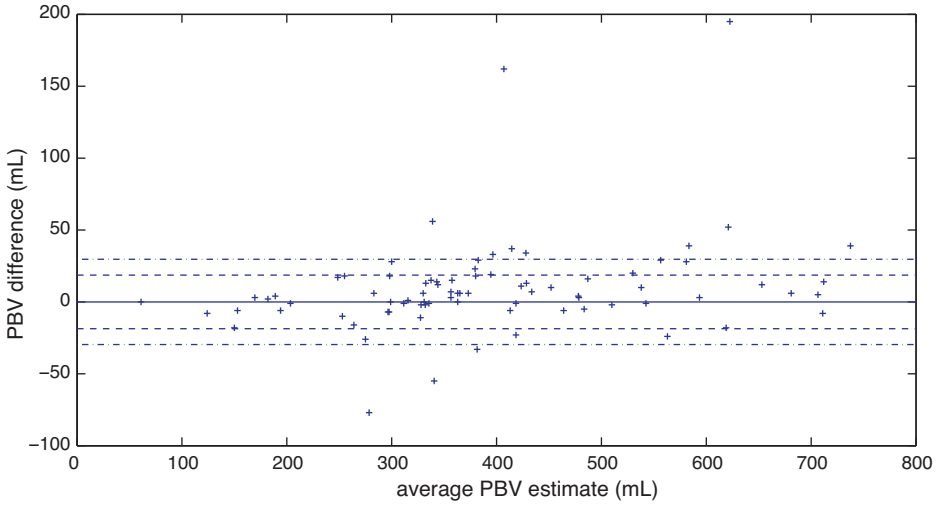

Fig. 6. Bland–Altman plot comparing the PBV estimates by LSE and LAD estimators in 80 measurements in patients. Dashed line indicates the mean and dash-dot line indicates the variance of the difference between LSE and LAD methods.

Comparison of MAD, SD, CC and Bias between Model-1 and Model-2, given in Tables 7 and 8, respectively, shows that Model-1 performs slightly better than Model-2.

Fig. 3 shows the estimates of EF by LSE, LAD and TLAD, plotted against bi-plane method and Fig. 4 shows the Bland–Altman analysis of bi-plane method with LSE, LAD and TLAD dilution methods [30].

The comparison of different EF measurement techniques shows significant standard deviations (usually of the order of 10–20%) [31]. The echocardiographic biplane method produces an EF underestimation with respect to magnetic resonance measurements (gold standard) [28]. Therefore, the EF overestimation by the model-based dilution methods with respect to the biplane method could effectively result in EF estimates that are closer to the gold standard.

The performance of PBV estimator is tested by using the data of the in-vitro experiment performed in [9]. In the in vitro set up, IDCs were measured before and after a capillary network whose volume is varied from 310 mL to 1080 mL by clamping different tubes. The flow is generated by a calibrated centrifugal pump (Medtronic 550 bioconsole) and an electromagnetic flowmeter embedded in the pump measures the flow. Flows ranging from 1 to 5 L/min were generated, in steps of 1 L/min. The estimated PBV values using LSE and LAD are shown in Fig. 5. The correlation coefficients with respect to the real volumes are 0.9955 and 0.9961 for LSE and LAD, respectively. The larger volumes (>1000 mL) are slightly underestimated by both the methods. However, volumes larger than 900 mL have never been measured in patients.

PBV estimation using LSE and LAD is performed in 80 of the 82 measurements collected in patients. In two patients, the RV window was not sufficient for IDC measurement. IDCs are denoised using a two stage TV-Rloess denoising. The results are shown in the Bland–Altman plot given in Fig. 6. The mean difference between LSE and LAD method is 18.6 mL and the standard deviation is 29.6 mL, which correspond to 4.7% and 7.5% of the average volume (average between the estimates of the two methods), respectively. These results confirm the feasibility of the measurements and their consistency across different implementations.

Table 8
MAD, SD, correlation and bias values of the error between EF estimates by biplane method and the parametric deconvolution method using LSE, LAD, MHFR HRF, TLAD, TLS estimators. Both LA and LV IDC are denoised using two stage TV-Rloess denoising method. All the EF estimates are based on Model-2.

	LAD	LSE	MHFR	HFR	TLAD	TLS
MAD	11.1365	12.5754	10.8934	11.2059	9.0227	10.8118
SD	15.0944	16.8342	14.7681	15.197	12.1845	14.8193
Corr	0.7174	0.6337	0.7105	0.7155	0.7076	0.6474
Bias	11.6473	12.575	11.4237	11.5661	6.4388	10.1751

6. Conclusions and future work

Estimation of EF and PBV using indicator dilution methods is studied, where we have used a parametric system identification technique to calculate EF and PBV. Two system models are proposed for the LV dilution system and one for the transpulmonary dilution system. Analysis of the two models (Model-1 and Model-2) proposed for EF estimation suggests that Model-1 approximates the LV dilution system better than Model-2.

Different estimators are proposed for estimating the LV and transpulmonary dilution system parameters and performance analysis of these estimators in assessing EF and PBV is done. In EF estimation, analysis of the results show that the LAD, HFR, MHFR and IRLS estimators perform better than the conventional LSE estimator. Since all the measured IDCs are corrupted by noise, TLS and TLAD are more suitable for system identification. Results given in Tables 3–7 show that the TLAD method, which accounts for measurement errors in both the input and the output IDCs, together with its robustness to outliers, is best suited for dilution system identification. In PBV estimation, only two estimators, LSE and LAD, are compared. In vitro results show that the LAD performs slightly better than LSE, but the difference is not significant.

The two stage denoising method, namely, TV-Rloess, proposed to denoise IDCs, gives significant improvement over single stage denoising methods, namely, FIR filtering and TV denoising in estimating EF and PBV.

6.1. Future work

The proposed dilution systems and the error functions for estimating EF and PBV requires a more extensive validation. EF estimates were compared with the bi-plane method, which is not a gold standard and has to be compared with magnetic resonance imaging method [31]. PBV estimates should be compared with transpolmunary dye or thermodilution measurements.

The values of regularization parameter, λ and local window length, l used in TV and Rloess denoising methods will effect the estimation of EF and PBV. In this paper, the values of λ and l are

found empirically and the same values are used for denoising all measured IDCs. Future work can also include a method to find the optimal values λ and l adaptively for each IDC. Finding the values of λ and l based on the IDC will prevent over or under smoothing of the IDCs and will therefore result in better EF and PBV estimation.

References

[1] H.J.C. Swan, W. Ganz, J. Forrester, H.M.G. Diamond, D. Chonette, Catheterization of the heart in man with use of a flow-directed balloon-tipped catheter, N. Engl. J. Med. 283 (1970) 447–451.

[2] S. Sakka, K. Reinhart, A. Meier-Hellmann, Comparison of pulmonary artery and arterial thermodilution cardiac output in critically ill patients, Intensive Care Med. 25 (1999) 843–846.

[3] J.D. Bronzino (Ed.), The Biomedical Engineering Handbook, 2nd ed., CRC Press, Boca Raton, 2000.

[4] X. Chen, K.Q. Schwarz, D. Phillips, S.D. Steinmetz, R. Schlief, A mathematical model for the assessment of hemodynamic parameters using quantitative contrast echocardiography, IEEE Trans. Biomed. Eng. 45 (6) (1998) 754–765.

[5] C.S. Sehgal, P.H. Arger, Mathematical modeling of dilution curves for ultrasonographic contrast, J. Ultrasound Med. 16 (1997) 471–479.

[6] P.J.A. Frinking, N. de Jong, Acoustic modeling of shell encapsuled gas bubbles, Ultrasound Med. Biol. 24 (4) (1998) 523–533.

[7] L. Hoff, Acoustic Caracterization of Contrast Agents for Medical Ultrasound Imaging, 1st ed., Kluwer Academica Publishers, Dordrecht, 2001.

[8] M. Mischi, A.A.C.M. Kalker, H.H.M. Korsten, Videodensitometric methods for cardiac output measurements, Eurasip J. Appl. Signal Process. 5 (2003) 479–489.

[9] M. Mischi, A.A.C.M. Kalker, H.H.M. Korsten, Contrast echocardiography for pulmonary blood volume quantification, IEEE Trans. Ultrasonics Ferroelectr. Freq. Control 51 (9) (2004) 1137–1147.

[10] M. Mischi, A.H.M. Jansen, A.A.C.M. Kalker, H.H.M. Korsten, Identification of ultrasound-contrast-agent dilution systems for ejection fraction measurements, IEEE Trans. Ultrason. Ferroelectr. Freq. Control 52 (3) (2005) 410–420.

[11] V. Uhlendorf, Physics of ultrasound contrast imaging: scattering in the linear range, IEEE Trans. Ultrason. Ferroelectr. Freq. Control 41 (1) (1994) 70–79.

[12] N. de Jong, A. Bouakaz, F.J.T. Cate, Contrast harmonic imaging, Ultrasonics 40 (1) (2002) 567–573.

[13] J.E. Chomas, P. Dayton, J. Allen, K. Morgan, K.W. Ferrara, Detection procedures of ultrasound contrast agents, IEEE Trans. Ultrason. Ferroelectr. Freq. Control 48 (1) (2001) 232–248.

[14] F.D. Scholle, V. Uhlendorf, T. Fritzsch, Physical mechanism of inhomogeneous left ventricular echocontrast, in: IEEE International Ultrasonics Symposium, IEEE UFFC Society, Montreal, (1994) pp. 13–16.

[15] M. Mischi, Contrast echocardiography for cardiac quantifications, Ph.D. thesis, Eindhoven University of Technology, 2004, available at http://www.sps.ele.tue.nl/members/M.Mischi/.

[16] M. Mischi, A.H.M. Jansen, A.A.C.M. Kalker, H.H.M. Korsten, Identification of cardiovascular dilution systems by contrast ultrasound, Ultrasound Med. Biol. 33 (3) (2007) 439–451.

[17] L. Huntsman, D. Stewart, S. Barnes, S. Franklin, J. Colocousis, E. Hessel, Noninvasive Doppler determination of cardiac output in man. clinical validation, Circulation 67 (1983) 593–602.

[18] C.M. Bishop, Pattern Recognition and Machine Learning, Springer, Singapore, 2006.

[19] P.W. Holland, R.E. Welsch, Robust regression using iteratively reweighted least-squares, Commun. Stat. Methods 6 (1977) 813–827.

[20] P.T. Boggs, J.E. Rogers, Orthogonal distance regression, in: Contemporary Mathematics, American Mathematical Society, 1990.

[21] A. Beck, M. Teboulle, Fast gradient-based algorithms for constrained total variation image denoising and deblurring problems, IEEE Trans. Image Process. 18 (11) (2009) 2419–2434.

[22] J.C. Lagarias, J.A. Reeds, M.H. Wright, P.E. Wright, Convergence properties of the Nelder–Mead simplex method in low dimensions, SIAM J. Optimiz. 9 (1) (1998) 112–147.

[23] W.S. Cleveland, Robust locally weighted regression and smoothing scatterplots, J. Am. Stat. Assoc. 74 (386) (1979) 829–836.

[24] A. Chambolle, Total variation minimization and a class of binary MRF models, Energy Minimiz. Methods Comput. Vision Pattern Recogn. 3757 (2005) 136–152.

[25] I. Selesnick, I. Bayram, Total variation filtering, Connexions Web site, 2009, http://cnx.org/content/m31292/1.1.

[26] M. Figueiredo, J. Bioucas-Dias, R. Nowa, Majorization–minimization algorithms for wavelet-based image restoration, IEEE Trans. Image Process. 16 (12) (2007) 2980–2991.

[27] A.H.M. Jansen, M. Mischi, F. Bracke, J.-M. van Dantzig, K. Peels, N. van Hemel, H.H.M. Korsten, Novel ultrasound-contrast-agent dilution method for assessment of ventricular ejection fraction, Eur. J. Echocardiogr. 9 (4) (2008) 489–493.

[28] S. Malm, S. Frigstad, E. Sagberg, H. Larsson, T. Skjaerpe, Accurate and reproducible measurement of ventricular volume and ejection fraction by contrast echocardiography, J. Am. Coll. Cardiol. 44 (5) (2004) 1030–1035.

[29] H.L. Thomson, A.J. Basmadjian, A.J. Rainbird, M. Razavi, J.F. Avierinos, P.A. Pellikka, K.R. Bailey, J.F. Breen, M. Enriquez-Sarano, Contrast echocardiography improves the accuracy and reproducibility of left ventricular remodeling measurements, J. Am. Coll. Cardiol. 38 (3) (2001) 867–875.

[30] J.M. Bland, D.G. Altman, Statistical methods for assessing agreement between two methods of clinical measurement, Lancet 327 (8476) (1986) 307–310.

[31] S. Schalla, E. Nagel, H.C.L.A.B. Klein, B. Schnackenburg, U. Schneider, E. Fleck, Comparison of magnetic resonance real-time imaging of left ventricular function with conventional magnetic resonance imaging and echocardiography, J. Am. Coll. Cardiol. 87 (2001) 95–99.